Temporal regulation of *Drosophila* IAP1 determines caspase functions in sensory organ development

Akiko Koto,[1] Erina Kuranaga,[1,2] and Masayuki Miura[1,2]

[1]Department of Genetics, Graduate School of Pharmaceutical Sciences, The University of Tokyo, Bunkyo-ku, Tokyo 113-0033, Japan
[2]Core Research of Evolutional Science & Technology, Japan Science and Technology Agency, Bunkyo-ku, Tokyo 113-0033, Japan

The caspases comprise a family of cysteine proteases that function in various cellular processes, including apoptosis. However, how the balance is struck between the caspases' role in cell death and their nonapoptotic functions is unclear. To address this issue, we monitored the protein turnover of an endogenous caspase inhibitor, *Drosophila* IAP1 (DIAP1). DIAP1 is an E3 ubiquitin ligase that promotes the ubiquitination of caspases and thereby prevents caspase activation. For this study, we developed a fluorescent probe to monitor DIAP1 turnover in the external sensory organ precursor (SOP) lineage of living *Drosophila*. The SOP divides asymmetrically to make the shaft, socket, and sheath cells, and the neuron that comprise each sensory organ. We found that the quantity of DIAP1 changed dramatically depending on the cell type and maturity, and that the temporal regulation of DIAP1 turnover determines whether caspases function nonapoptotically in cellular morphogenesis or cause cell death.

Introduction

Programmed cell death, or apoptosis, is essential for normal animal development, as well as cell fate determination, proliferation, and differentiation. Studies in the worm, fly, and mammals have shown that the molecular mechanisms regulating apoptosis are well conserved. In programmed cell death, members of the caspase family of cysteine proteases are activated and cleave diverse substrates to destroy the structure of the cells. Mechanisms that control caspase activation are essential for maintaining cell integrity, and the inhibitor of apoptosis proteins (IAPs), originally found in baculoviruses, carry out this function. In *Drosophila*, loss-of-function mutations in the gene *thread (th)*, which encodes *Drosophila* IAP1 (DIAP1), result in early embryonic death through the inappropriate activation of apoptosis (Wang et al., 1999; Goyal et al., 2000; Rodriguez et al., 2002). DIAP1 contains a C-terminal RING finger domain and functions as an E3 ubiquitin ligase. It suppresses caspase activation by binding directly to caspases and promoting their degradation or nondegradative inactivation (Ditzel et al., 2008) through polyubiquitylation. During periods of programmed cell death, DIAP1 degradation is promoted by the proapoptotic proteins Reaper (Rpr), Head involution defective (Hid), and Grim. When caspases are released from DIAP1 inhibition, programmed cell death is executed. Therefore, the balance between the DIAP1 protein level and caspase activation determines whether cells will survive or die by apoptosis.

Recent studies have revealed that cell death signaling components also execute nonapoptotic functions (for review see Kuranaga and Miura, 2007; Yi and Yuan, 2009). Caspase activity is required for a variety of developmental events, including sperm individualization (Arama et al., 2003; Huh et al., 2004), antennal aristae formation (Cullen and McCall, 2004), border cell migration (Geisbrecht and Montell, 2004), neural cell-fate decisions (Kanuka et al., 2005; Kuranaga et al., 2006), and dendrite pruning (Kuo et al., 2006; Williams et al., 2006). However, the regulatory mechanisms that permit the caspases to carry out nonapoptotic functions while preventing apoptosis remain largely unknown.

Evidence exists for at least two mechanisms that permit a cell to activate caspase safely for nonapoptotic functions. One mechanism involves sequestering the caspase activity in specific subcellular regions (Arama et al., 2003; Huh et al., 2004;

Correspondence to Masayuki Miura: miura@mol.f.u-tokyo.ac.jp

Abbreviations used in this paper: APF, after puparium formation; DIAP1, *Drosophila* inhibitor of apoptosis protein 1; DmIKKε, *Drosophila* IKK-related kinase; IAP, inhibitor of apoptosis protein; MARCM, mosaic analysis with a repressive cell marker; SOP, sensory organ precursor.

The Rockefeller University Press $30.00
J. Cell Biol. Vol. 187 No. 2 219–231
www.jcb.org/cgi/doi/10.1083/jcb.200905110

Kuo et al., 2006; Williams et al., 2006). An evidence for this comes from the observation that, during dendrite pruning, caspase activity is restricted to dendrites that are going to be severed, but is not seen in the soma or axon (Kuo et al., 2006; Williams et al., 2006). Another proposed mechanism is that the activity of the caspase cascade, when carrying out nonapoptotic functions, is too weak to destroy the cell. This has been reported as a likely mechanism for the caspase function in neural cell fate determination (Kanuka et al., 2005; Kuranaga et al., 2006), in which low caspase activity is required to regulate the Wingless signaling pathway, which contributes to the emergence of neural precursor cells.

In this study, we provide evidence for a third regulatory mechanism for nonapoptotic caspase activity: temporal regulation. To investigate the nonapoptotic functions and regulatory mechanisms of the caspases, we focused on the protein dynamics of DIAP1. A mechanism of DIAP1 turnover in nonapoptotic status is known: DIAP1 is directly phosphorylated by *Drosophila* IKK-related kinase (DmIKKε), which promotes it for degradation. In addition, DmIKKε-mediated DIAP1 turnover affects nonapoptotic functions of caspases, such as *Drosophila* neural precursor development (Kuranaga et al., 2006) and cellular morphogenesis, including the dendrite pruning (Lee et al., 2009), and the formation of *Drosophila* antennal aristae and sensory bristles (Oshima et al., 2006; and this paper). Moreover, because DIAP1 has a RING finger domain and functions as an E3 ubiquitin ligase, the metabolism of the DIAP1 protein is very likely to be critical for the temporal and quantitative control of caspases. However, little evidence has been gathered about DIAP1 protein dynamics in vivo.

To detect dynamic changes in DIAP1 levels, we developed a fluorescent probe and performed a live-imaging analysis that revealed DIAP1 turnover and functions throughout the process of sensory organ development. Sensory organs on the thorax are formed by four cells: one shaft, socket, and sheath cell, and one neuron. These cells arise from four rounds of asymmetric cell division by the sensory organ precursor (SOP) cell (Gho et al., 1999; Reddy and Rodrigues, 1999). A glial cell is also generated; however, it undergoes nuclear fragmentation shortly after its birth and dies (Fichelson and Gho, 2003). Thus, the SOP lineage is a good model system for studying the mechanisms of cell fate determination, proliferation, differentiation, and cell death. Our detailed analysis of DIAP1 turnover during sensory organ development showed that, depending on the cell differentiation state, DIAP1 executes two distinct functions, one in the survival of the shaft cell, and one in its morphogenesis; both functions are exerted through the regulation of caspase activity. Thus, the precise temporal control of DIAP1 degradation is critical to keep the balance between cellular structural integrity and the execution of caspase's nonapoptotic functions.

Results

Indicator for DIAP1 degradation: PRAP

To make DIAP1 protein turnover visible in living cells, we generated a fusion protein of mutated DIAP1 and Venus, a modified YFP (Nagai et al., 2002). For successful live-imaging analysis with such fluorescent probes, there are some factors we should be making certain: one is that the expression of the probe does not disturb the endogenous signaling, and the other is that the probe can mimic the protein turnover of endogenous protein, as the protein stability or its degradation pathway. Because DIAP1 directly binds to and inhibits the *Drosophila* caspase-9 (Dronc) (Hawkins et al., 2000; Meier et al., 2000; Quinn et al., 2000) and caspase-3 (drICE and DCP-1) homologues (Kaiser et al., 1998; Hawkins et al., 1999) through its baculovirus IAP repeat (BIR) domains, a DIAP1 fusion protein could suppress endogenous signaling when ectopically expressed. To circumvent this problem, we introduced into the DIAP1 construct two point mutations that are reported to block DIAP1's ability to bind caspases (Fig. 1 A). Specifically, we used the mutations in $th^{11\text{-}3e}$, a loss-of-function DIAP1 allele that fails to bind activated drICE and DCP-1 (Zachariou et al., 2003) and in th^{4}, which is also a loss-of-function allele with a single amino acid mutation (H283Y) in the BIR2 domain and shows impaired binding to pro-Dronc (Wilson et al., 2002). We named this probe PRAP (pre-apoptosis signal detecting probe based on DIAP1 degradation).

PRAP expression does not disturb cell death signaling

We first examined whether PRAP disturbed caspase signaling by comparing its effects with those of the wild-type DIAP1-Venus fusion protein. In *Drosophila* S2 cells, Reaper-induced cell death was suppressed by DIAP1-Venus in a dose-dependent manner; however, PRAP did not suppress cell death at all (Fig. 1 B). In addition, the Reaper-induced small eye phenotype (Fig. 1 D) was not rescued by PRAP (Fig. 1 F), but the expression of DIAP1 or DIAP1-Venus markedly improved it (Fig. 1, C and E). We also confirmed that PRAP expression did not have any effect on the Hid-induced small eye phenotype (unpublished data). These results show that PRAP does not disturb caspase-dependent cell death signaling when it is overexpressed in vivo.

PRAP is as unstable as endogenous DIAP1

DIAP1 degradation depends on the ubiquitin–proteasome pathway, and DIAP1 has a half-life of ∼30 min (Wilson et al., 2002; Yoo et al., 2002). To determine the half-life of PRAP, we performed cycloheximide chase experiments in S2 cells expressing PRAP, and confirmed that the half-life of both PRAP and endogenous DIAP1 was ∼30 min (Fig. 1 G). This result also suggests that PRAP expression does not disturb the protein turnover of endogenous DIAP1 and does not have a dominant-negative effect.

Next, to test whether the ubiquitin–proteasome pathway regulated the turnover of the PRAP protein, cells expressing PRAP were treated with lactacystin, a specific and irreversible inhibitor of the 20S and 26S proteasome. Lactacystin treatment enhanced the amount of PRAP protein, as well as that of the endogenous DIAP1 protein (Fig. 1 H), showing that PRAP was also degraded by the ubiquitin–proteasome pathway. These experiments confirmed that the amount of PRAP was regulated by the same mechanisms as endogenous DIAP1.

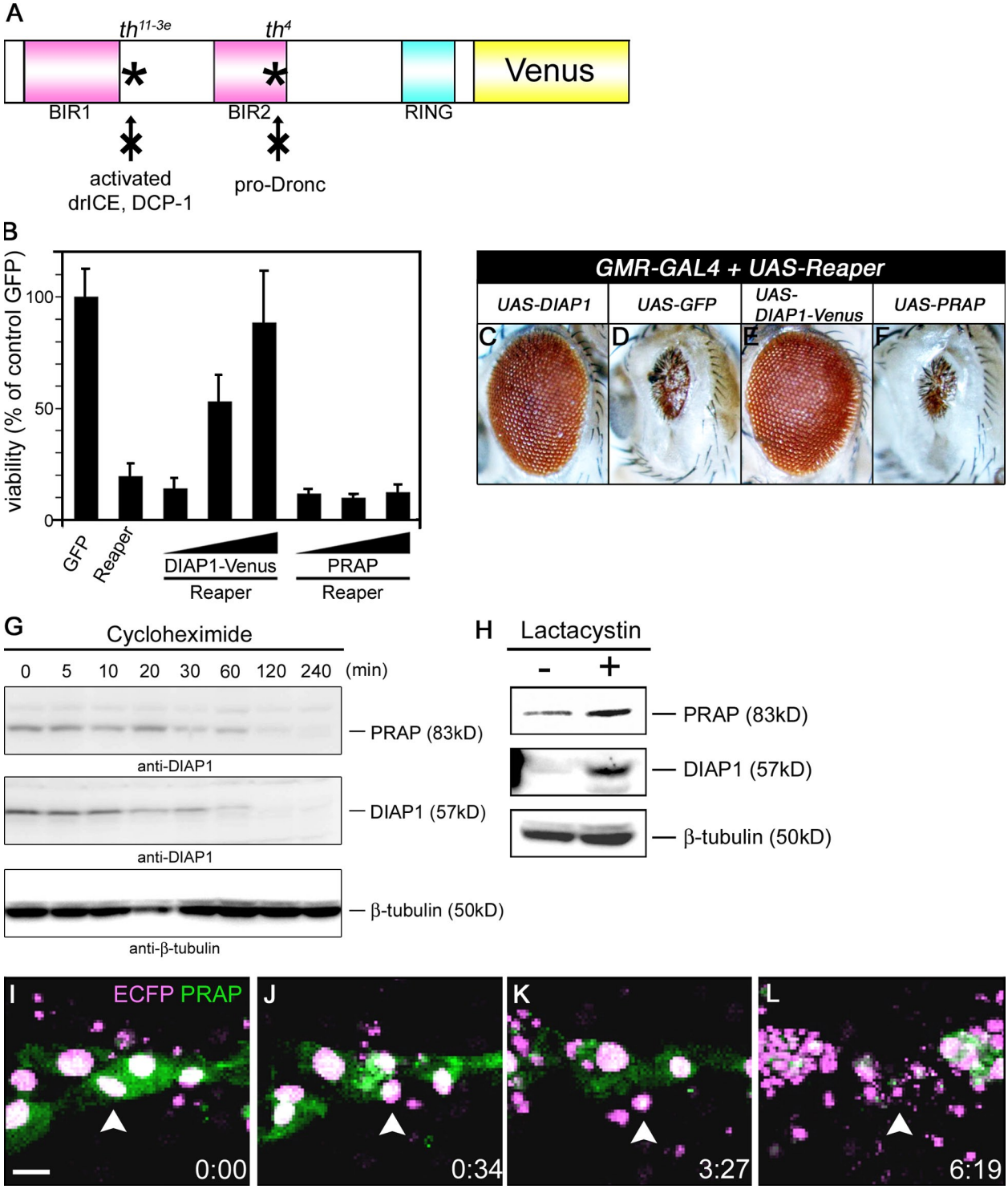

Figure 1. **Development and characterization of PRAP, a fluorescent probe for monitoring DIAP1 degradation.** (A) Schematic representation of PRAP. (B) Cell death was not inhibited by PRAP expression in S2 cells. Cell viability (mean ± SD) was determined by a cell death assay 36 h after transfection with each indicator (1, 5, or 15 ng), 5 ng of *pUAST-Reaper*, and 10 ng of *pWAGAL4* together with 100 ng of *pCaSperR-hs-lacZ*. (C–F) Eye phenotype of *UAS-mycDIAP1/+; UAS-Reaper/+; GMR-GAL4/+* (C), *UAS-Reaper/UAS-GFP; GMR-GAL4/+* (D), *UAS-Reaper/UAS-DIAP1-Venus; GMR-GAL4/+* (E), and *UAS-Reaper/UAS-PRAP; GMR-GAL4/+* (F). (G) PRAP is an unstable protein with a short half-life. S2 cells were treated with cycloheximide, and cell extracts were prepared at the times indicated. The expression levels of PRAP and the endogenous DIAP1 protein were detected in whole-cell lysates by immunoblotting with an anti-DIAP1 antibody. (H) PRAP degradation is mediated by the ubiquitin–proteasome pathway. 18 h after S2 cells were transfected with 20 ng of *pUAST-PRAP* and 5 ng of *pWAGAL4*, the cells were divided into two dishes and incubated for 5 h with or without lactacystin. The levels of PRAP and endogenous DIAP1 protein were detected by immunoblotting with an anti-DIAP1 antibody. (I–L) PRAP (green) is degraded before the nuclear condensation and morphological changes that accompany cell death. Arrowhead indicates a cell showing PRAP degradation. To mark each nucleus, the ECFP signal is shown in magenta. Bar, 20 μm. The genotype was *en-GAL4 UAS-PRAP/+; UAS-Histone2B-ECFP/+*.

PRAP mirrors DIAP1 degradation in times of physiological cell death

Because it was confirmed that PRAP could be degraded by the expression of proapoptotic protein, Reaper, in a dose-dependent manner in S2 cells (Fig. S1), next we examined the protein turnover of PRAP when physiological cell death is induced in vivo. Here, we focused on the replacement of the abdominal epithelial cell sheet during metamorphosis because its histology is well studied, and it can easily be observed by live imaging (Ninov et al., 2007). Larval epidermal cells (LECs) undergo cell death, and adult epidermis replaces the LECs during the pupal stage. Both PRAP and a nuclear marker, Histone2B-ECFP, were expressed in the LECs using the *engrailed-GAL4* driver. First, we monitored PRAP fluorescence in the LECs (Fig. 1 I). As metamorphosis progressed, we saw that rapid PRAP degradation soon followed (Fig. 1 J); after PRAP disappeared, the epithelial nuclei condensed, and the LECs were removed from the epithelial sheet (Fig. 1, K and L). These results showed that PRAP could be used to monitor the protein turnover of endogenous DIAP1 in physiological programmed cell death. Therefore, we concluded that PRAP signal mirrors the stability of endogenous DIAP1 and allows us to monitor temporal dynamics of DIAP1 at high resolution in real time, in vivo.

DIAP1 turnover during sensory organ development

We next focused on the development of sensory organs, called microchaetes, on the notum. Microchaetes are studied as typical structures of the *Drosophila* peripheral nervous system. They are formed by two outer support cells (the socket cell and the shaft cell) and two inner cells (the neuron and the sheath cell) (Fig. 2 A), which all arise from asymmetric divisions of the sensory organ precursor (SOP or pI [i.e., precursor I]) cell (Fig. 2 B). Live imaging of pupae during a 20-h period beginning 16 h after puparium formation (APF) allowed us to follow the development of the entire bristle lineage, from the pI cell to bristle elongation.

We used the *neuralized* driver (*neu-GAL4*) to express *UAS-PRAP* and a *UAS-Histone2B-ECFP*, specifically in the SOP lineage. We observed a dynamic degradation pattern of PRAP that differed in each cell of the SOP lineage (Fig. 2, C–S; and Video 1). PRAP was detected in the pI cell at the beginning of our observation at 16 h APF (Fig. 2, C and M). The PRAP signal persisted in the pIIa and pIIb daughter cells (Fig. 2, D and N), but disappeared from them before the pIIb cell divided (Fig. 2 E). During the next cell division of pIIb, PRAP was not detected in the pIIa, pIIIb, or the glial cell (Fig. 2 F). The next cell division of pIIa produces the socket and shaft cells. During this time, PRAP was never observed in pIIIb, pIIa, or the socket or shaft cells (Fig. 2 G). The final division of pIIIb produces the neuron and sheath cell, and these cells were also negative for PRAP (Fig. 2 H). After this final cell division and the death of the glial cell (Fig. 2, H and I, white arrowheads), PRAP fluorescence reemerged in the socket cell and the shaft cell (Fig. 2, J, K, O, and P). Later in development, just before the beginning of bristle elongation, PRAP rapidly vanished from the shaft cell (Fig. 2, L and Q, yellow arrowheads).

Because the intensity of the Histone2B-ECFP signal (Fig. 2, C–L) and other fluorescent probes, such as mCD8-GFP or SCAT3 (Takemoto et al., 2003), did not change during sensory organ development (unpublished data), this cell type– and time-dependent degradation pattern was specific to PRAP. The same pattern of PRAP dynamics was observed when *UAS-PRAP* was driven by the *scabrous-GAL4* driver (*sca-GAL4*), which expresses GAL4 strongly in the SOP and its descendants (unpublished data), indicating that the observed dynamics did not depend on the promoter activity of the GAL4 driver. Finally, we confirmed that the endogenous DIAP1 protein was likewise distributed asymmetrically after the final cell division (compare Fig. 2 T with Fig. 2 K), indicating that endogenous DIAP1 is regulated post-translationally and that PRAP mirrors the changes in the endogenous DIAP1 protein dynamics.

The observation of PRAP dynamics in wild-type flies yielded two unexpected findings. First, PRAP was degraded to the point of extinguishing its fluorescence between the 2-cell stage of sensory organ development and the 5-cell stage (Fig. 2, E–I). This was surprising because DIAP1, as a cell death inhibitor, is thought to be essential for cell survival during development. Second, our finding that the amount of PRAP protein was different in each cell type suggested that DIAP1 degradation could be determined by the cell type (Fig. 2, J–L, S; and Fig. S2).

We wondered why cells in the SOP lineage could survive without DIAP1. To find out, we used SCAT3, a FRET indicator for the activity of effector caspases (Takemoto et al., 2003, 2007), and found that effector caspases were activated in the glial cell, when it died, but not in the other SOP progeny (Fig. S3 A). We also found that *dark/dapaf-1/hac-1*, the *Drosophila* homologue of Apaf-1, which promotes activation of the initiator caspase Dronc, was not detectable in the SOP lineage, except for the glial cell (Fig. S3 B).

Dynamic changes in the DIAP1 level depend on the cell type

To investigate further the apparent dependence of the PRAP stability on cell fate, we next used live-imaging analysis of *numb* mutant clones, generated by the MARCM (mosaic analysis with a repressive cell marker) system (Lee and Luo, 1999). Numb specifies the fate of SOP progeny by inhibiting Notch activity in the daughter cell to which it is asymmetrically segregated (Rhyu et al., 1994; Guo et al., 1996). In the *numb* mutant, the pIIb cell is transformed into an ectopic pIIa cell, and the most common phenotype of the *numb* mutant is three socket cells and one shaft cell (Fig. 3 K).

In the SOP lineage within the *numb* mutant clones, PRAP degradation was observed during cell division in the same pattern as in the wild-type lineage (Fig. 3, A–D). However, after the final cell division, PRAP started to accumulate in all four cells (Fig. 3, E, G, and H) and was degraded only later, in the shaft cell, just before bristle elongation (Fig. 3, F, I, and J, arrowheads). In the other three cells, which developed into sockets, PRAP fluorescence did not diminish (Fig. 3, F, I, and J). These results suggest that in cells adopting an alternate fate, PRAP mirrors the protein turnover seen in the wild-type cells of the same fate.

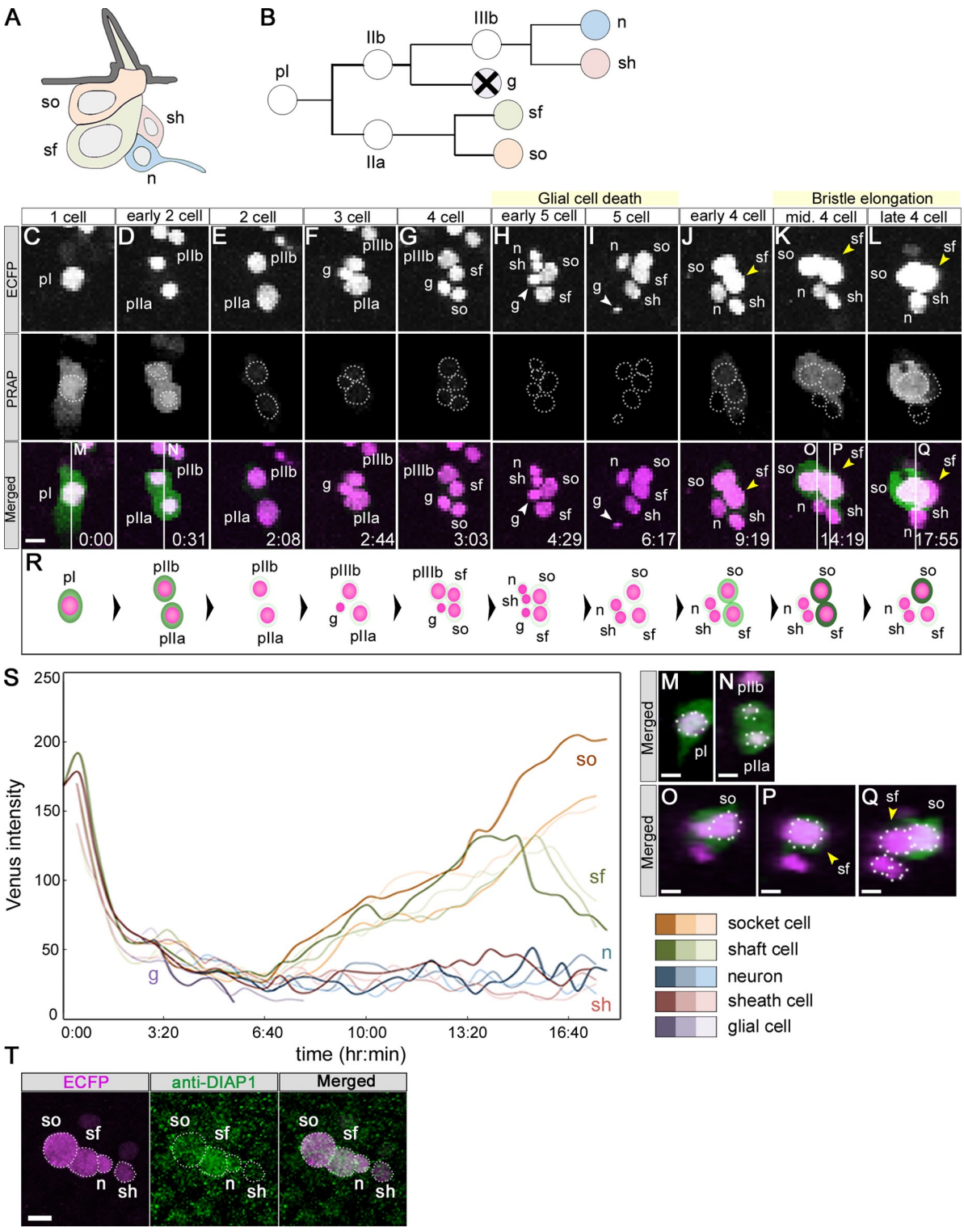

Figure 2. **DIAP1 dynamics in the SOP lineage.** (A) External sensory organ. Sensory organs are formed by two external cells, the shaft (sf) and the socket (so) cells, and two inner cells, the internal neuron (n) and the sheath (sh) cell. (B) The SOP lineage. The progenitor cells, pI, pIIa, pIIb, and pIIIb (white) divide to form the five cells of the external sensory organ shown in A. The socket and shaft cells arise from the pIIa cell. The neuron, sheath, and glial (g) cells arise from the pIIb lineage. The glial cell soon dies by apoptosis. (C–L) PRAP protein dynamics in the SOP lineage at progressive stages of development. In vivo live-imaging analysis of PRAP (green) was begun at ~16 h APF. The time course of the imaging analysis is shown at the bottom right of the merged panel. Glial cell death is indicated by white arrowheads. Note that in the shaft cell (yellow arrowheads) PRAP vanishes acutely before bristle elongation. Each nucleus is marked by Histone2B-ECFP (magenta) and is outlined by a dashed line. (M–Q) Panels are Y-Z sections of the cells shown in C, D, K, and L. pI cell shown in C corresponds to the cell in M. pIIa and pIIb cells in D correspond to N. The socket cell in K was shown in O, and the shaft cell in K was in P. Both socket and shaft cell in L was indicated in Q. Bar, 5 μm. (R) Schematic representation of PRAP dynamics from a pI cell (i.e., SOP cell) to bristle formation. (S) Sequential variation of Venus intensity in each cell type (so, orange; sf, green; n, blue; sh, red; g, purple). Three representative lineages are shown. (T) Endogenous DIAP1 protein is regulated post-translationally. The endogenous DIAP1 protein was detected in the socket and shaft cells, after the final precursor cell division. Bar, 5 μm. The genotype was *neu-GAL4 UAS-Histone2B-ECFP/UAS-PRAP39*.

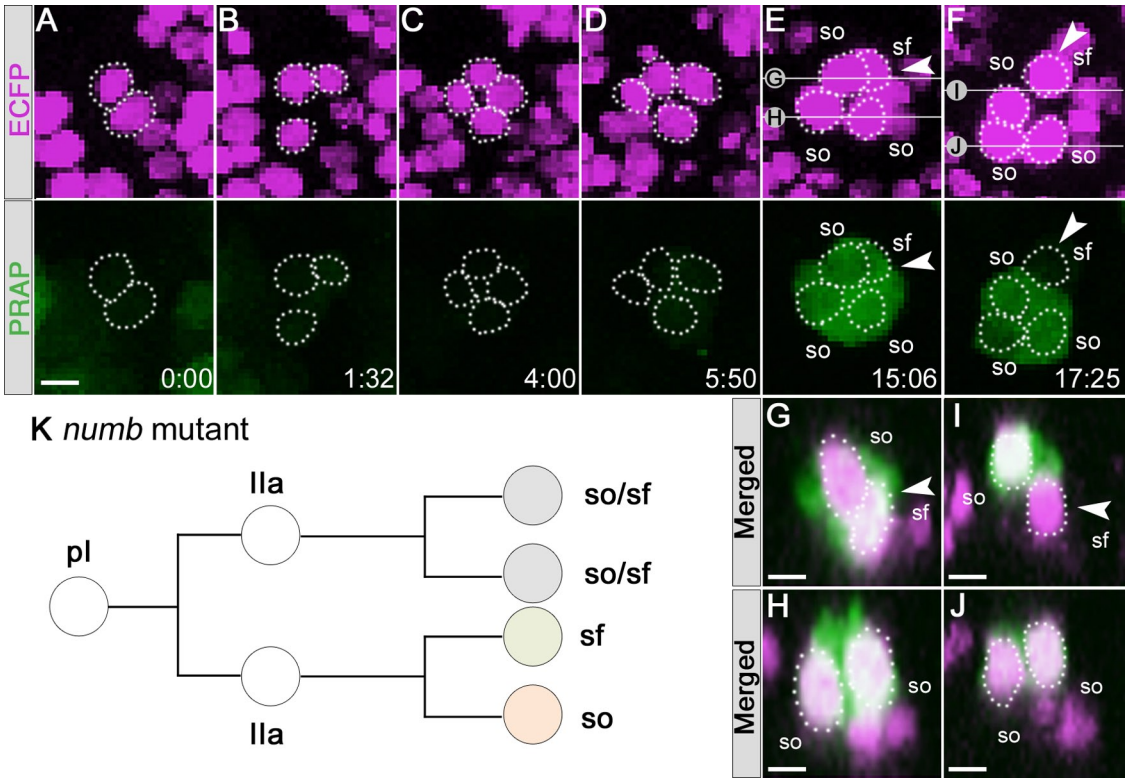

Figure 3. **DIAP1 dynamics depend on cell type.** In *numb*^{2} mutant clones, PRAP dynamics changed with cells' transformation to a new fate. (A–F) The PRAP pattern was dependent on cell fate. PRAP accumulation was observed in all four cells after cell division, and it was degraded only in the shaft cell (E and F, arrowheads). The final fate of the cells was confirmed by examining the outer morphology, after the imaging analysis. The *numb*^{2} mutant clone is marked by Histone2B-ECFP (magenta) and PRAP (green) expression. Dashed lines outline the nuclei. (G–J) Merged images of cross sections shown in E and F. Bar, 5 µm. (K) The *numb*^{2} mutant causes the transformation of a pIIb cell into an ectopic pIIa cell. The genotype was *Ubx-flp/+; y*$^+$ *numb*^{2} *ck FRT40A/tub-GAL80 FRT40A; neu-GAL4 UAS-Histone2B-ECFP/UAS-PRAP22*.

DIAP1 accumulation in the shaft cell affects bristle morphogenesis

Because this was the first evidence that the amount of DIAP1 protein changes dramatically in the normal developmental context, we next studied the physiological significance of DIAP1 dynamics during sensory organ development. We tried manipulating the *diap1* level to see the effects on sensory organ development. First, we examined PRAP stability and the adult bristle phenotype in *H99* mutant MARCM clones, which lack the genomic region containing *reaper*, *hid*, and *grim*. In these clones, the PRAP degradation pattern was normal, and bristle morphology was completely unaffected (unpublished data). This observation, together with the result that PRAP could be degraded by Reaper expression (Fig. S1), suggested that proapoptotic proteins (RHG proteins) may not be involved in the regulation of DIAP1 during sensory organ development.

Next, we tested the development of the SOP lineage of the *DmIKKε* knock-down fly because DmIKKε down-regulates the DIAP1 protein level through direct phosphorylation (Kuranaga et al., 2006). In this knock-down line, PRAP was degraded in the same manner as in the wild-type SOP lineage (unpublished data), but with delayed timing in the shaft cell, in which the PRAP signal was strong even after the start of bristle elongation (Fig. 4 C). In the wild-type lineage, PRAP was never observed during bristle elongation (Fig. 4 A). Furthermore, we observed that the bristles were shorter and thicker in the adult notum of the *DmIKKε* knock-down fly (Fig. 4 D) than in the wild-type fly (Fig. 4 B), as reported previously (Oshima et al., 2006).

To investigate the relationship between PRAP turnover and bristle morphology, we compared the bristle length in lineages showing normal PRAP degradation in the shaft cell with the length in lineages with delayed PRAP degradation in the shaft cell; both lineage types could be observed in the same *DmIKKε* knock-down fly. In lineages showing normal PRAP degradation, the bristle length was 65.4 ± 3.46 µm (n = 34; Fig. 4 E). In those showing delayed PRAP degradation, the bristles were significantly shorter (53.9 ± 4.76 µm, n = 7; Fig. 4 E). These results indicate that the delayed degradation of PRAP in the shaft cell is related to the formation of a short bristle. We next looked for genetic interactions between *diap1* and *DmIKKε*. We found that the overexpression of DIAP1 enhanced the short-bristle phenotype of the *DmIKKε* knock-down line (Fig. 4 F), suggesting that DIAP1 is involved in the morphogenesis of the shaft cell, and that DmIKKε regulates the timing of DIAP1 protein degradation during bristle elongation. Because the bristle length of a fly overexpressing DIAP1 in an otherwise wild-type fly was 71.6 ± 0.62 µm (Fig. 4 F), the same as wild-type (69.5 ± 1.18 µm; Fig. 4 F), DIAP1 must induce the short-bristle phenotype synergistically with DmIKKε.

We also found that coexpression of a dominant-negative form of Dronc in the *DmIKKε* knock-down flies significantly enhanced the short-bristle phenotype, just as DIAP1 overexpression did

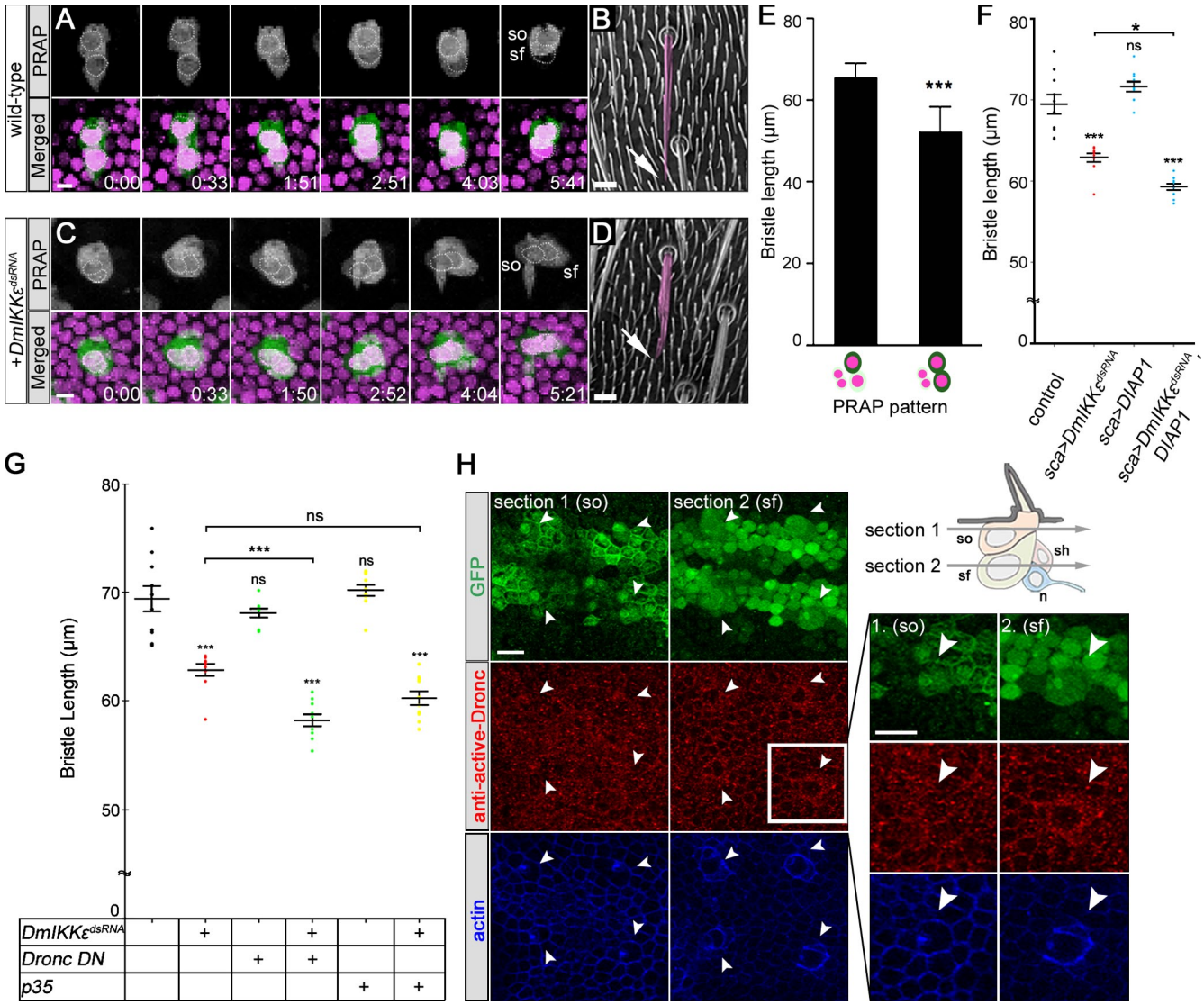

Figure 4. ***DmIKKε* knock-down alters the DIAP1 degradation pattern and impairs morphogenesis of the shaft cell.** (A) PRAP dynamics in the wild-type SOP lineage. Dashed lines outline the nuclei. Bar, 5 μm. (B) External adult bristles in a wild-type fly. Bar, 10 μm. The tip of a bristle is indicated by a white arrow. (C) In the *DmIKKε* knock-down SOP lineage, PRAP degradation is delayed, and PRAP is still detectable after bristle elongation starts. (D) Microchaetes of the *DmIKKε* knock-down flies are shorter and thicker than the wild-type bristles shown in B. (E) Bristle length (mean ± SD) is significantly shorter in lineages with delayed PRAP degradation (53.4 ± 4.76 μm; $n = 7$) than in lineages showing the normal PRAP pattern (65.4 ± 3.46 μm; $n = 34$). The P value was calculated using an unpaired two-tailed Student's *t* test. ***, $P < 0.0001$. (F) Genetic interaction between *diap1* and *DmIKKε* in shaft cell formation. *DmIKKε* was reduced by *DmIKKε*^{dsRNA}. DIAP1 level was enhanced by the overexpression of myc-tagged DIAP1. (G) Effects of DmIKKε, Dronc, and drICE/DCP-1 on shaft-cell formation. The average bristle lengths in individual flies are plotted ($n = 10$ flies). Asterisks indicate statistical significance compared with control, as determined by one-way ANOVA with Tukey's HSD post-hoc analysis. *, $P < 0.05$; ***, $P < 0.001$; n.s., not significant. Data are shown as the mean ± SEM. (H) Dronc was activated in the shaft cell during bristle elongation. The processed form of Dronc was detected using an antibody specific for activated Dronc. The socket cell (section 1) and shaft cell (section 2) are shown. Arrowheads indicate the positions of the socket or shaft cells in each section. Bar, 10 μm. Genotypes: *sca-GAL4 UAS-PRAP/+; UAS-Histone2B-ECFP/+* (A), *sca-GAL4 UAS-PRAP/+; UAS-Histone2B-ECFP/UAS-IR2615* (C and E), and *sca-GAL4/UAS-GFP* (H).

(Fig. 4 G). In addition, in wild-type flies, Dronc activation detected by anti-active Dronc antibody seemed to be stronger in the cytoplasmic region of the shaft cell than that of the socket cell (Fig. 4 H, Figs. S4 and S5). These observations, together with the timing of PRAP turnover in wild-type flies (Fig. 2), suggested that the degradation of DIAP1 promotes Dronc activation in the shaft cell, allowing it to execute its nonapoptotic function in bristle formation.

Interestingly, the coexpression of baculovirus p35, which is commonly used to inhibit the activation of effector caspases (DCP-1 and drICE), results in the short bristles in *DmIKKε* knock-down fly; however, there was no statistical difference about the bristle length, compared with only *DmIKKε* knock-down flies (Fig. 4 G). Additionally, the activation of effector caspases was not observed in either the socket or the shaft cell during bristle formation, using SCAT3 imaging analysis (unpublished data). Therefore, despite the activation of Dronc, drICE and DCP-1 seem not to be involved in shaft formation. We expect that as the shaft cell differentiates and matures, it acquires a mechanism for suppressing the activation of effector caspases. DIAP2 is a

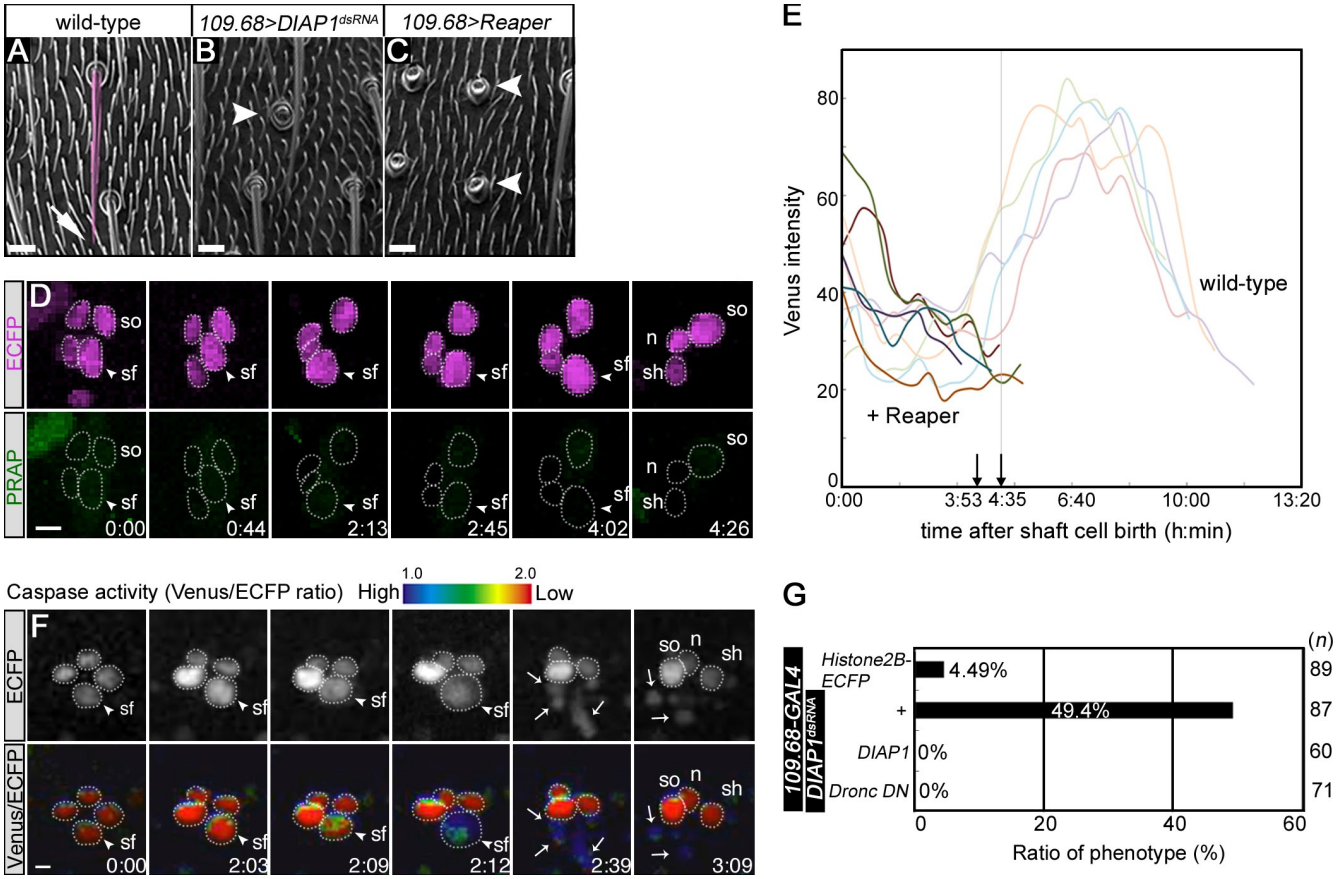

Figure 5. **DIAP1 functions as a caspase inhibitor in the early stage of shaft cell differentiation.** (A) Wild-type bristle. (B and C) Down-regulation of the *diap1* level induces a loss-of-bristle phenotype. The sockets (arrowheads) were present and only the bristles were missing. Bars, 10 µm. (D) In the Reaper-expressing SOP lineage, PRAP did not accumulate at detectable levels in the socket or shaft cells, and the shaft cell eventually migrated away. Arrowheads indicate the shaft cell. Dashed lines outline the cell nuclei. (E) The sequential variation of Venus intensity in the shaft cell of the Reaper-expressing SOP lineage (dark lines) and the wild-type SOP lineage (faint lines). The time of the shaft cell's birth was defined as 0:00. The shaft cell disappeared 4:35 ± 0:58 h (mean ± SD) after its birth, accompanied by rapid PRAP degradation (n = 18). In the wild-type lineage, PRAP accumulation starts 3:53 ± 1:18 h (n = 13) after the cell's birth. Five representative lines from each genotype are shown. (F) Caspase activation is observed in the shaft cell before its nuclear fragmentation (arrows). Caspase activity was examined by the imaging of a FRET-based probe, nls-SCAT3, and shown in pseudocolor. Arrowheads indicate the shaft cell, and fragmented nuclei are indicated by arrows. Bar, 5 µm. (G) Genetic interaction of DIAP1^{dsRNA}-expressing flies with cell death signaling components. The loss-of-bristle phenotype was completely rescued by the dominant-negative form of Dronc. *109.68-GAL4 UAS-DIAP1-IR/CyO* flies were crossed to flies with the indicated genotypes. The number of F1 progeny adult flies exhibiting at least one loss-of-bristle lineage on the notum was counted, and the percentage (%) was calculated. The sample number (n) is indicated at the right side of each bar. The genotypes were as follows: w^{1118} (A), *109.68-GAL4 UAS-DIAP1-IR/CyO* (B), *109.68-GAL4/UAS-Reaper* (C), *109.68-GAL4/UAS-Reaper; UAS-PRAP/UAS-Histone2B-ECFP* (D, and +Reaper in E), *109.68-GAL4/+; UAS-PRAP/UAS-Histone2B-ECFP* (wild-type in E), *109.68-GAL4/*UAS-Reaper*; UAS-nls-SCAT3/+* (F). The genotypes of flies used in G were as follows: *109.68-GAL4/UAS-Histone2B-ECFP* (*Histone2B-ECFP*), *109.68-GAL4 UAS-DIAP1-IR/CyO* (+), *UAS-mycDIAP1/+; 109.68-GAL4 UAS-DIAP1-IR/+* (*DIAP1*), *109.68-GAL4 UAS-DIAP1-IR/+; UAS-Dronc DN/+* (*Dronc DN*).

specific inhibitor for drICE (Ribeiro et al., 2007). We found that PRAP stability and the morphology of the adult sensory organ were not affected in *diap2* mutant flies, suggesting that DIAP2 was not involved in the resistance against the killing activity of caspases in the sensory organ lineage (unpublished data); however, there must be other mechanisms for suppressing the activation of effector caspases and being resistant to the cell-killing activity of Dronc.

Stabilization of DIAP1 is essential for survival of the shaft cell

Although drICE and DCP-1 were not activated in the absence of DIAP1 before the terminal differentiation of the shaft cell (Fig. S3 A), immediately after the final cell division, Dronc activation was required for proper elongation of the shaft (Fig. 4, G and H). This transient stage of Dronc activation might be dangerous for the shaft cell. We speculated that an accumulation of DIAP1 after the final cell division is required to balance the caspase activity to allow the execution of its nonapoptotic function and avoid cell death. To test this possibility, we examined the effect of down-regulating *diap1*. The knock-down of *diap1* using the *109.68-GAL4* driver, which expresses GAL4 in all four cells of the adult sensory organ, resulted in the loss of bristles, but sockets showed normal development (Fig. 5 B). To down-regulate the endogenous DIAP1 protein, we next expressed Reaper ectopically, and found that only the bristles were lost on the adult notum (Fig. 5 C), indicating a defect in only the shaft cell. A detailed analysis using live imaging revealed that in the SOP lineages that expressed Reaper, the SOP divided four times, just as in the wild-type lineage, made the same five cell types,

and showed the same developmental time course, beginning 16 h APF (unpublished data). However, after the final cell division the PRAP level never became high enough to be detected, and it was never observed, even in the socket or shaft cell. The Reaper-expressing shaft cell began to migrate away soon after its birth (Fig. 5 D, arrowheads), and it disappeared 4 h 35 min (± 58 min) later (n = 18; Fig. 5 E). In addition, the activation of effector caspases and nuclear fragmentation (Fig. 5 F, arrows), typical signs of apoptosis, were observed in the shaft cell (Fig. 5 F), and the loss-of-bristle phenotype of DIAP1^{dsRNA} was completely rescued by the expression of dominant-negative Dronc (Fig. 5 G). These results suggested that when *diap1* was down-regulated after the final cell division in the shaft cell, effector caspases were inappropriately activated, causing the cell to die.

In contrast, the socket, neuron, and sheath cells survived even with Reaper overexpression, suggesting that these cells have mechanisms for maintaining their structural integrity and suppressing caspase activation without DIAP1. It was interesting that effector caspases were activated in only the shaft cell when Reaper was ectopically expressed. Presumably, after the final cell division, the shaft cell enters a fragile state in which Dronc expression begins and the cell is equipped for the execution of Dronc's nonapoptotic functions in bristle formation (Fig. 6). During this stage, DIAP1 stabilization is essential to maintain cell integrity and to keep the level of caspase activation in the shaft cell low. Thus, the timing of DIAP1 degradation is critical for allowing the nonapoptotic functions of Dronc in cell shape formation to occur while protecting the cell from apoptosis.

Discussion

DIAP1 was first reported as a cell death inhibitor that works by suppressing caspase activation; other physiological functions of DIAP1 have been reported more recently (for review see Kuranaga and Miura, 2007; Yi and Yuan, 2009). Although the physiological importance of DIAP1 has been stressed in various cellular events, little has been known about the regulation of its turnover. Our analysis of DIAP1 turnover in the living animal has shed new light on the physiological roles and the regulatory mechanisms of cell death signaling components, including the caspases. To do this analysis, we developed a novel reporter protein for monitoring DIAP1 turnover, PRAP. Because PRAP is the fusion protein of mutated DIAP1 and Venus, its turnover may not be perfectly the same with the endogenous DIAP1 protein turnover. However, as far as we tested, PRAP turnover mirrored the protein dynamics of endogenous DIAP1 (Fig. 1 and Fig. S1). The observation of PRAP dynamics in living animals provides us the insight to investigate in vivo the spatial and temporal pattern of DIAP1 protein expression.

One of the most absorbing questions about the nonapoptotic roles of the caspases is how caspase activity is regulated so that it does not induce programmed cell death. Until recently, the regulatory mechanism of programmed cell death has been thought to be simple, that is, to obey an all-or-nothing law that depends on the activation of caspases. For example, when caspase is released from inhibition by DIAP1 and activated, cells die. However, in the case of caspase's nonapoptotic functions, the mechanisms appear to be more complicated and delicate. In this study, we found that DIAP1 degradation was regulated in a cell lineage– and stage-specific manner and that the time-course of caspase activation depended on that of DIAP1 protein turnover. Our findings supported the hypothesis that, to execute its nonapoptotic functions, caspase has to be activated only when cells have acquired resistance to the killing activity of the cell death signaling components.

The other proposed mechanism is that the caspases are activated only in controlled subcellular locations (Arama et al., 2003; Kuo et al., 2006; Williams et al., 2006). For example, caspase activation is involved in dendrite pruning during *Drosophila* metamorphosis (Kuo et al., 2006; Williams et al., 2006), and its activation is observed only in dendrites at the point where they will subsequently be severed, but not in the axon, soma, or nucleus. In spermatogenesis, the spermatid bulk cytoplasm is eliminated by caspase activation (Arama et al., 2003; Huh et al., 2004). Arama et al. (2003) found that, during this process, the nucleus is protected from the killing activity of caspases by the expression of dBruce, a giant ubiquitin-conjugating enzyme that is thought to inhibit apoptosis. In *dbruce* mutants, spermatid nuclei become highly condensed and degenerate. In this case, too, the spatial restriction of caspase activity and of the IAPs is essential to maintain the safety of the cell. In addition, modulation of the strength of caspase activation is critical for it to execute its nonapoptotic functions. Low caspase activity contributes to neural cell-fate determination in *Drosophila* sensory organ development (Kanuka et al., 2005). It has been unclear how the localization and the strength of caspase activation are regulated in vivo. The mechanism we describe here, that the modulation of DIAP1 protein turnover regulates caspase activation to permit nonapoptotic functions of cell death signaling components, could also be involved in other strategies for nonapoptotic caspase functions, including the spatial restriction of activated caspases and the control of their activation levels.

By observing PRAP stability in the *Drosophila* sensory organ lineage, we learned that DIAP1 degradation did not always result in caspase activation and cell death. We propose that there are two different cell states that determine cellular sensitivity to apoptosis. One is exhibited by cells that can survive without DIAP1, as the shaft cell does in phases I and III (Fig. 6); the other is exhibited by cells that cannot survive without DIAP1 expression, as seen in the shaft cell in phase II. One explanation for a cell's ability to survive without DIAP1 is that other, unknown mechanisms exist to defend the cell from caspase activation. Some anti-apoptotic defense mechanisms have been described in other developmental systems. Recently, the epigenetic control of proapoptotic genes was shown to regulate cellular sensitivity to cell death signals in *Drosophila* embryos, so that they were dramatically less sensitive to irradiation between 7 and 9 h after egg laying (Zhang et al., 2008). That study showed that the epigenetic silencing of *reaper* and *hid* expression is essential for the sensitive-to-resistant transition. In addition, the suppression of *hid* mRNA translation by maternal Nanos is indispensable for pole-cell survival in *Drosophila* embryos (Sato et al., 2007).

In this study, *dapaf-1* expression seemed to be reduced in phase I, which might have contributed to the inhibition of

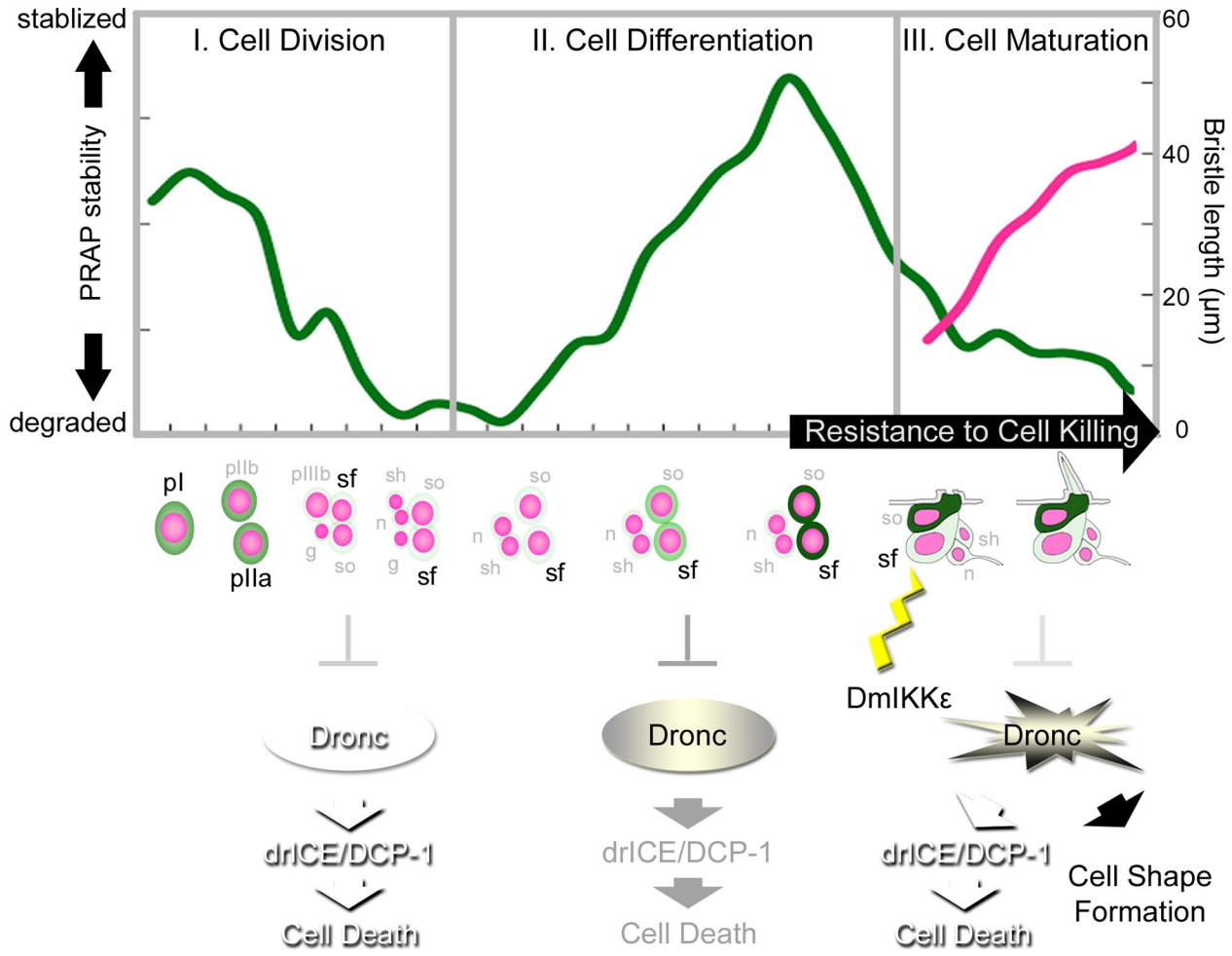

Figure 6. **Schematic representation of shaft cell development and DIAP1 protein dynamics.** DIAP1 degradation is sustained during SOP cell division (phase I) and induced again just before bristle elongation (phase III). In the middle phase (phase II), Dronc could be activated in the absence of DIAP1, indicating that DIAP1 functions as a cell death inhibitor to suppress caspase activation and maintain the cellular integrity. In phase III, DIAP1 needs to be degraded with specific timing to regulate shaft cell morphogenesis appropriately. PRAP expression dynamics are shown in green and bristle length as a magenta line.

caspase activity. This observation is consistent with findings from several other systems, including the adult rat brain (Yakovlev et al., 2001; Ota et al., 2002) and neuronally differentiated PC12 cells (Wright et al., 2004), in that neuronal differentiation is accompanied by a marked reduction in Apaf-1, resulting in a significant decrease in caspase activity. Because the neuron and sheath cells survived without DIAP1 throughout sensory organ development, these cells probably acquired some mechanism to suppress executioner caspase activation at the time of their terminal differentiation.

After the terminal differentiation, sensory bristles are formed by the extension of shaft cells to the animal's exterior, accompanied by the assembly of a small cluster of F-actin filaments, close to the membrane of the growing tip (Tilney et al., 1995). The short and thick bristle phenotype of the *DmIKKε* down-regulated flies suggests that DIAP1 contributes to the regulation of the actin cytoskeleton in the sensory organ lineage, especially in the initial step of actin assembly or actin polymerization. Previous reports showed the involvement of cell death signaling components in regulating actin cytoskeleton (Oshima et al., 2006; Shapiro and Anderson, 2006; Lee et al., 2009). Our results validate the idea that a DmIKKε–DIAP1 signaling pathway is involved in cellular morphogenesis during *Drosophila* development. Moreover, we found that the initiator caspase Dronc is involved in this process, but drICE and DCP-1 are not (Fig. 4, G and H). The same observation has been made for border cell migration (Geisbrecht and Montell, 2004), the formation of antenna aristae (Oshima et al., 2006), and dendrite pruning (Kuo et al., 2006; Lee et al., 2009) in *Drosophila*. However, the downstream targets of Dronc have remained elusive. Presumably, some Dronc substrates function as critical effectors for the nonapoptotic roles of Dronc regulating cellular morphogenesis.

Another remaining issue is the physiological significance of DIAP1 degradation in phase I. There is some evidence that the IAP family plays integral roles in cell division, most notably in cytokinesis. For example, although overexpression of the *Caenorhabditis elegans* IAP homologue BIR-1 cannot suppress cell death, its reduction by RNA interference induces a cytokinesis defect (Fraser et al., 1999). Furthermore, both XIAP and survivin, the mammalian IAPs, can affect mitotic processes because the transient overexpression of XIAP induces cell cycle

arrest (Levkau et al., 2001), and the disruption of survivin function by the antisense cDNA alters the centrosome and leads to multipolar mitoses (Li et al., 1999). Here, we tried to manipulate the DIAP1 dyamics using the *H99* mutant MARCM clone (unpublished data) and *DmIKKε* down-regulation (Fig. 4, C–E); however, its degradation pattern was not disturbed in phase I, suggesting that there may be one or more other regulators of DIAP1 turnover during SOP cell division. Further study will be required to pinpoint the physiological function of DIAP1 in the regulation of cell division and cytokinesis during the asymmetric divisions of the SOP cell.

Our live-imaging analysis of DIAP1 dynamics provides an opportunity to study its apoptotic and nonapoptotic functions in a developmental context that allows caspases to execute their nonapoptotic functions.

Materials and methods

Gene construction

To construct PRAP, a mutated *diap1* cDNA was amplified from *BSSK-DIAP1*, using the following primers, which contain the necessary point mutations: CGCACTACCAACAAGGTGCCGATCAAT and CCCTGGGAACAGTACGCTCTCTGGCTA. The wild-type *diap1* and mutant cDNAs were amplified using the following primers: forward, 5′-CCGGAATTCGCCGCCACCATGGCATCTGTTGTAGCTGAT-3′; reverse, 5′-CCCAAGCTTGCTGCCGCCGCTGCCGCCAGAAAAATATACGCGCATCAC-3′. The resulting PCR products were ligated into the EcoRV site of the BSSK vector. The cDNA encoding Venus was amplified using the following primers: forward, 5′-CCCAAGCTTGGCGGCAGCGGCGGCAGCATGGTGAGCAAGGGCGAGGAG-3′; reverse, 5′-CTAGTCTAGATTACTTGTACAGCTCGTCCAT-3′. The amplified product was ligated into the EcoRV site of the BSSK vector. The *diap1* and mutated *diap1* fragments were released by digestion with EcoRI–HindIII, and the Venus cDNA by digestion with HindIII–XbaI. The fragments were gel purified and ligated into the EcoRI–XbaI site of *pUAST* to generate *pUAST-DIAP1-Venus* and *pUAST-PRAP*.

To construct *pUAST-Dronc-wt* and *pUAST-Dronc-E352A*, Dronc-wt or Dronc-E352A cDNAs were isolated from the plasmid *pET32a-dronc (wt)* or *pET32a-dronc (E352A)* (provided by L. Dorstyn and S. Kumar, Hanson Institute, Adelaide, Australia) as the NdeI–NotI fragment and cloned into the EcoRI and NotI site of *pUAST*.

Fly stocks, transgenic flies, and clonal analysis

Flies were raised on standard *Drosophila* medium at 25°C, and the transgenic strains were described previously (Kanuka et al., 1999). The following fly strains were used in this study: *GMR-GAL4 (III)*, *en-GAL4*, *neu-GAL4*, *109.68-GAL4*, *UAS-GFP (S65T)*, *A101* (Bloomington *Drosophila* Stock Center, Bloomington, IN); *sca^{P309}-GAL4* (Reddy and Rodrigues, 1999); *UAS-IR2615* (Oshima et al., 2006); *UAS-DIAP1* (Hay et al., 1995); *UAS-p35*, *UAS-Reaper* (Zhou et al., 1997); *UAS-Dronc DN* (Quinn et al., 2000); *UAS-DIAP1-IR* (Genetics Strain Research Center, National Institute of Genetics, Shizuoka, Japan); *UAS-Histone2B-ECFP* (provided by S. Kondo, The University of Tokyo, Tokyo, Japan); and *UAS-nls-SCAT3/MKRS* (provided by Y. Nakajima, The University of Tokyo, Tokyo, Japan). Mosaic clones of *numb* were made by using FRT40A-recombined alleles of *numb^2*. *Ubx-flp* (Hutterer and Knoblich, 2005), *y$^+$ numb^2 ck FRT40A, p(tub)gal80 FRT40A* flies were provided by Y.N. Jan (University of California, San Francisco, San Francisco, CA), and the procedure was described previously (Justice et al., 2003).

Cell culture, transfections, cell death assays, and immunoblotting

The *Drosophila* S2 cell culture, cell death assay, and immunoblotting were performed as described previously (Kuranaga et al., 2002). The primary antibodies were rabbit anti-DIAP1 (1:1,000; Kuranaga et al., 2006) and mouse anti–β-tubulin (1:500, Promega; to detect the loading control). For the cell death assay, S2 cells in a 24-well plate were transiently transfected with 1, 5, or 15 ng of *pUAST-DIAP1-Venus* and 1, 5, or 15 ng of *pUAST-PRAP*; 5 ng of *pUAST-Reaper*; 10 ng of *pWAGAL4*; and 100 ng of *pCaSpeR-hs-lacZ*. As the positive control, S2 cells were transfected with 20 ng of *pUAST-GFP* and 10 ng of *pWAGAL4*. The relative amount of each protein was determined by densitometric analysis using Image Gauge software (Fujifilm). Quantitative data were obtained as the ratio of the indicated protein signal to that of the loading control for each immunoblot and were plotted as a ratio graph.

Treatment with proteasome inhibitor and cycloheximide

The experimental procedure was described previously (Kuranaga et al., 2006). Lactacystin (20 μM; EMD) was used as the proteasome inhibitor. S2 cells in a 6-well plate were transiently transfected with 5 ng of *pWAGAL4* and 20 ng of *pUAST-PRAP*. For the cycloheximide (CHX) treatment, S2 cells were transfected with 5 ng of *pCaSpeR-hs-GAL4* and 50 ng of *pUAST-PRAP*. Cycloheximide was added at 50 μg/ml.

Preparation of living pupae and image acquisition

Staged pupae were washed in water and mounted on a glass slide using double-sided tape. The pupal case covering the entire abdomen or notum was removed. Very wet filter paper was placed around the pupae to keep them hydrated. The pupae were covered with a cover-glass in a small drop of water, to avoid desiccation. Silicon (Shinetsu) was used to seal the chamber. Live imaging with PRAP was performed on a Pascal confocal microscope (Carl Zeiss, Inc) with a 40x NA 1.3 Plan Neofluar oil immersion objective (Carl Zeiss, Inc.) or 20x NA 0.5 Plan Neofluar objective (Carl Zeiss, Inc.) at 22°C, using LSM software (Carl Zeiss, Inc). Live imaging for FRET was performed on a microscope (DM 6000B; Leica) equipped with a CSU10 confocal unit (Yokogawa) and cooled CCD camera (Coolsnap HQ; Photometrics, Roper) at 22°C, using an HCX PL 40x NA1.25–0.75 oil immersion objective (Leica), and the image acquisition and analyses were performed using MetaMorph software (MDS Analytical Technologies). Photoshop (CS3; Adobe) was used to adjust brightness and contrast. In most cases, the animal survived during the data acquisition and developed into an adult.

Histology

For the scanning electron microscopy, we used model VE-8800 (KEYENCE). For light microscopy of the adult fly eye, flies were anaesthetized and examined with a microscope (model MZ16F; Leica) equipped with a digital camera (model DC480; Leica).

In situ hybridization and immunohistochemistry

Immunochemistry of the pupal notum was performed as described previously (Sato et al., 1999b). Simultaneous staining for protein and RNA was performed using the original protocol (Sato et al., 1999a). *dapaf-1* antisense RNA probes were prepared by in vitro transcription with a 1.8-kb BamHI–XhoI fragment of *dapaf-1* cDNA as the template (Kanuka et al., 1999). Because it was reported that autoprocessing at TQTE containing E352 is important for Dronc activation (Muro et al., 2004; Dorstyn and Kumar, 2008), a specific antibody against the processed form of Dronc was raised in rabbit using a synthetic peptide, PDTQTE, conjugated with keyhole limpet hemocyanin as the immunogen, and was purified by affinity purification and used for immunostaining (1:100). The following antibodies were used for immunostaining in this study: mouse anti–β-gal (1:100; Promega), anti-GFP (1:500; Aves Laboratories), anti–chick IgY FITC (1:500; Jackson ImmunoResearch Laboratories, Inc.), Alexa Fluor 633–phalloidin (1:100; Invitrogen), anti–rabbit IgG Cy3 (1:100; Jackson ImmunoResearch Laboratories, Inc.), anti–mouse IgG Alexa Fluor 488 (1:100; Invitrogen), anti–rabbit IgG Cy5 (1:100; Jackson ImmunoResearch Laboratories, Inc.), and anti–DIG-Rhodamine (1:1,500; Roche). Fixed samples shown in Fig. 2 T were imaged with a confocal microscope (Pascal; Carl Zeiss, Inc), with a 40x NA 1.3 Plan Neofluar oil immersion objective (Carl Zeiss, Inc.) and LSM software (Carl Zeiss, Inc). Immunohistochemistry shown in Fig. 4 H was performed with a confocal microscope (model TCS SP5; Leica) using an HCX PL 40x NA1.25–0.75 oil immersion objective (Leica) and Application Suite Advanced Fluorescence software (Leica).

Statistical analysis and quantification

The groups were compared using unpaired two-tailed Student's *t* test in Fig. 4 E, and using a one-way analysis of variance (ANOVA) with Tukey's HSD post-hoc analysis in Fig. 4, F and G, using PRISM software (version 5.0a; GraphPad Software, Inc.). To quantify the bristle length of microchaete in adult flies, flies were dissected and were transferred to a drop of Hoyer's medium on slide glass. After the cuticle preparation, bristle lengths were measured by Qwin software (Leica).

Online supplemental material

Fig. S1 shows that PRAP could be degraded by Reaper expression. Fig. S2 shows the sequential variation of PRAP intensity in each cell type of SOP lineage. Fig. S3 shows that PRAP degradation does not result in caspase

activation in the SOP lineage. Fig. S4 shows the characterization of anti-active Dronc antibody. Fig. S5 shows Dronc activation in the shaft cell during bristle elongation. Video 1 shows the PRAP pattern in the SOP lineage. Online supplemental material is available at http://www.jcb.org/cgi/content/full/jcb.200905110/DC1.

We thank H. Steller, L. Dorstyn, S. Kumar, Y.N. Jan, R. Ueda, S. Kondo, and Y. Nakajima for fly strains and materials, and the Bloomington *Drosophila* Resource Center, the *Drosophila* Genetic Resource Center (Kyoto Institute of Technology, Kyoto, Japan), and the Genetics Strain Research Center for fly strains. We especially thank K. Takemoto for the generous suggestions and support for the live-imaging analysis, and to all the members of the Miura laboratory for valuable discussions. We are grateful to H. Kanuka for kind support and encouragement, and T. Chihara and Y. Yamaguchi for helpful advice and critical reading of this manuscript. We thank S. Hayashi for critical reading of this manuscript and helpful discussion, and M. Sato for technical support. We thank the University of Tokyo and Leica Microsystems Imaging Center (TLI) for imaging analysis.

This work was supported by grants from the Japanese Ministry of Education, Science, Sports, Culture and Technology (to M. Miura and E. Kuranaga) and by grants from the Astellas Foundation for Metabolic Disorders (to M. Miura), the Naito Foundation (to M. Miura and E. Kuranaga), and the Cell Science Research Foundation (to M. Miura); a RIKEN Bioarchitect research grant (to M. Miura), the Uehara Memorial Foundation (to E. Kuranaga), the Kanae Foundation for the Promotion of Medical Science (to E. Kuranaga), and the Takeda Science Foundation (to E. Kuranaga). A. Koto is a research fellow of the Japan Society for the Promotion of Science.

Submitted: 20 May 2009
Accepted: 23 September 2009

References

Arama, E., J. Agapite, and H. Steller. 2003. Caspase activity and a specific cytochrome C are required for sperm differentiation in *Drosophila*. *Dev. Cell.* 4:687–697. doi:10.1016/S1534-5807(03)00120-5

Cullen, K., and K. McCall. 2004. Role of programmed cell death in patterning the *Drosophila* antennal arista. *Dev. Biol.* 275:82–92. doi:10.1016/j.ydbio.2004.07.028

Ditzel, M., M. Broemer, T. Tenev, C. Bolduc, T.V. Lee, K.T. Rigbolt, R. Elliott, M. Zvelebil, B. Blagoev, A. Bergmann, and P. Meier. 2008. Inactivation of effector caspases through nondegradative polyubiquitylation. *Mol. Cell.* 32:540–553. doi:10.1016/j.molcel.2008.09.025

Dorstyn, L., and S. Kumar. 2008. A biochemical analysis of the activation of the *Drosophila* caspase DRONC. *Cell Death Differ.* 15:461–470. doi:10.1038/sj.cdd.4402288

Fichelson, P., and M. Gho. 2003. The glial cell undergoes apoptosis in the microchaete lineage of *Drosophila*. *Development.* 130:123–133. doi:10.1242/dev.00198

Fraser, A.G., C. James, G.I. Evan, and M.O. Hengartner. 1999. *Caenorhabditis elegans* inhibitor of apoptosis protein (IAP) homologue BIR-1 plays a conserved role in cytokinesis. *Curr. Biol.* 9:292–301. doi:10.1016/S0960-9822(99)80137-7

Geisbrecht, E.R., and D.J. Montell. 2004. A role for *Drosophila* IAP1-mediated caspase inhibition in Rac-dependent cell migration. *Cell.* 118:111–125. doi:10.1016/j.cell.2004.06.020

Gho, M., Y. Bellaïche, and F. Schweisguth. 1999. Revisiting the *Drosophila* microchaete lineage: a novel intrinsically asymmetric cell division generates a glial cell. *Development.* 126:3573–3584.

Goyal, L., K. McCall, J. Agapite, E. Hartwieg, and H. Steller. 2000. Induction of apoptosis by *Drosophila* reaper, hid and grim through inhibition of IAP function. *EMBO J.* 19:589–597. doi:10.1093/emboj/19.4.589

Guo, M., L.Y. Jan, and Y.N. Jan. 1996. Control of daughter cell fates during asymmetric division: interaction of Numb and Notch. *Neuron.* 17:27–41. doi:10.1016/S0896-6273(00)80278-0

Hawkins, C.J., S.L. Wang, and B.A. Hay. 1999. A cloning method to identify caspases and their regulators in yeast: identification of *Drosophila* IAP1 as an inhibitor of the *Drosophila* caspase DCP-1. *Proc. Natl. Acad. Sci. USA.* 96:2885–2890. doi:10.1073/pnas.96.6.2885

Hawkins, C.J., S.J. Yoo, E.P. Peterson, S.L. Wang, S.Y. Vernooy, and B.A. Hay. 2000. The *Drosophila* caspase DRONC cleaves following glutamate or aspartate and is regulated by DIAP1, HID, and GRIM. *J. Biol. Chem.* 275:27084–27093.

Hay, B.A., D.A. Wassarman, and G.M. Rubin. 1995. *Drosophila* homologs of baculovirus inhibitor of apoptosis proteins function to block cell death. *Cell.* 83:1253–1262. doi:10.1016/0092-8674(95)90150-7

Huh, J.R., S.Y. Vernooy, H. Yu, N. Yan, Y. Shi, M. Guo, and B.A. Hay. 2004. Multiple apoptotic caspase cascades are required in nonapoptotic roles for *Drosophila* spermatid individualization. *PLoS Biol.* 2:E15. doi:10.1371/journal.pbio.0020015

Hutterer, A., and J.A. Knoblich. 2005. Numb and alpha-Adaptin regulate Sanpodo endocytosis to specify cell fate in *Drosophila* external sensory organs. *EMBO Rep.* 6:836–842. doi:10.1038/sj.embor.7400500

Justice, N., F. Roegiers, L.Y. Jan, and Y.N. Jan. 2003. Lethal giant larvae acts together with numb in notch inhibition and cell fate specification in the *Drosophila* adult sensory organ precursor lineage. *Curr. Biol.* 13:778–783. doi:10.1016/S0960-9822(03)00288-4

Kaiser, W.J., D. Vucic, and L.K. Miller. 1998. The *Drosophila* inhibitor of apoptosis D-IAP1 suppresses cell death induced by the caspase drICE. *FEBS Lett.* 440:243–248. doi:10.1016/S0014-5793(98)01465-3

Kanuka, H., K. Sawamoto, N. Inohara, K. Matsuno, H. Okano, and M. Miura. 1999. Control of the cell death pathway by Dapaf-1, a *Drosophila* Apaf-1/CED-4-related caspase activator. *Mol. Cell.* 4:757–769. doi:10.1016/S1097-2765(00)80386-X

Kanuka, H., E. Kuranaga, K. Takemoto, T. Hiratou, H. Okano, and M. Miura. 2005. *Drosophila* caspase transduces Shaggy/GSK-3beta kinase activity in neural precursor development. *EMBO J.* 24:3793–3806. doi:10.1038/sj.emboj.7600822

Kuo, C.T., S. Zhu, S. Younger, L.Y. Jan, and Y.N. Jan. 2006. Identification of E2/E3 ubiquitinating enzymes and caspase activity regulating *Drosophila* sensory neuron dendrite pruning. *Neuron.* 51:283–290. doi:10.1016/j.neuron.2006.07.014

Kuranaga, E., and M. Miura. 2007. Nonapoptotic functions of caspases: caspases as regulatory molecules for immunity and cell-fate determination. *Trends Cell Biol.* 17:135–144. doi:10.1016/j.tcb.2007.01.001

Kuranaga, E., H. Kanuka, T. Igaki, K. Sawamoto, H. Ichijo, H. Okano, and M. Miura. 2002. Reaper-mediated inhibition of DIAP1-induced DTRAF1 degradation results in activation of JNK in *Drosophila*. *Nat. Cell Biol.* 4:705–710. doi:10.1038/ncb842

Kuranaga, E., H. Kanuka, A. Tonoki, K. Takemoto, T. Tomioka, M. Kobayashi, S. Hayashi, and M. Miura. 2006. *Drosophila* IKK-related kinase regulates nonapoptotic function of caspases via degradation of IAPs. *Cell.* 126:583–596. doi:10.1016/j.cell.2006.05.048

Lee, H.H., L.Y. Jan, and Y.N. Jan. 2009. *Drosophila* IKK-related kinase Ik2 and Katanin p60-like 1 regulate dendrite pruning of sensory neuron during metamorphosis. *Proc. Natl. Acad. Sci. USA.* 106:6363–6368. doi:10.1073/pnas.0902051106

Lee, T., and L. Luo. 1999. Mosaic analysis with a repressible cell marker for studies of gene function in neuronal morphogenesis. *Neuron.* 22:451–461. doi:10.1016/S0896-6273(00)80701-1

Levkau, B., K.J. Garton, N. Ferri, K. Kloke, J.R. Nofer, H.A. Baba, E.W. Raines, and G. Breithardt. 2001. xIAP induces cell-cycle arrest and activates nuclear factor-kappaB : new survival pathways disabled by caspase-mediated cleavage during apoptosis of human endothelial cells. *Circ. Res.* 88:282–290.

Li, F., E.J. Ackermann, C.F. Bennett, A.L. Rothermel, J. Plescia, S. Tognin, A. Villa, P.C. Marchisio, and D.C. Altieri. 1999. Pleiotropic cell-division defects and apoptosis induced by interference with survivin function. *Nat. Cell Biol.* 1:461–466. doi:10.1038/70242

Meier, P., J. Silke, S.J. Leevers, and G.I. Evan. 2000. The *Drosophila* caspase DRONC is regulated by DIAP1. *EMBO J.* 19:598–611. doi:10.1093/emboj/19.4.598

Muro, I., K. Monser, and R.J. Clem. 2004. Mechanism of Dronc activation in *Drosophila* cells. *J. Cell Sci.* 117:5035–5041. doi:10.1242/jcs.01376

Nagai, T., K. Ibata, E.S. Park, M. Kubota, K. Mikoshiba, and A. Miyawaki. 2002. A variant of yellow fluorescent protein with fast and efficient maturation for cell-biological applications. *Nat. Biotechnol.* 20:87–90. doi:10.1038/nbt0102-87

Ninov, N., D.A. Chiarelli, and E. Martín-Blanco. 2007. Extrinsic and intrinsic mechanisms directing epithelial cell sheet replacement during *Drosophila* metamorphosis. *Development.* 134:367–379. doi:10.1242/dev.02728

Oshima, K., M. Takeda, E. Kuranaga, R. Ueda, T. Aigaki, M. Miura, and S. Hayashi. 2006. IKK epsilon regulates F actin assembly and interacts with *Drosophila* IAP1 in cellular morphogenesis. *Curr. Biol.* 16:1531–1537. doi:10.1016/j.cub.2006.06.032

Ota, K., A.G. Yakovlev, A. Itaya, M. Kameoka, Y. Tanaka, and K. Yoshihara. 2002. Alteration of apoptotic protease-activating factor-1 (APAF-1)-dependent apoptotic pathway during development of rat brain and liver. *J. Biochem.* 131:131–135.

Quinn, L.M., L. Dorstyn, K. Mills, P.A. Colussi, P. Chen, M. Coombe, J. Abrams, S. Kumar, and H. Richardson. 2000. An essential role for the caspase dronc in developmentally programmed cell death in *Drosophila*. *J. Biol. Chem.* 275:40416–40424. doi:10.1074/jbc.M002935200

Reddy, G.V., and V. Rodrigues. 1999. A glial cell arises from an additional division within the mechanosensory lineage during development of the microchaete on the *Drosophila* notum. *Development.* 126:4617–4622.

Rhyu, M.S., L.Y. Jan, and Y.N. Jan. 1994. Asymmetric distribution of numb protein during division of the sensory organ precursor cell confers distinct fates to daughter cells. *Cell.* 76:477–491. doi:10.1016/0092-8674(94)90112-0

Ribeiro, P.S., E. Kuranaga, T. Tenev, F. Leulier, M. Miura, and P. Meier. 2007. DIAP2 functions as a mechanism-based regulator of drICE that contributes to the caspase activity threshold in living cells. *J. Cell Biol.* 179:1467–1480. doi:10.1083/jcb.200706027

Rodriguez, A., P. Chen, H. Oliver, and J.M. Abrams. 2002. Unrestrained caspase-dependent cell death caused by loss of Diap1 function requires the *Drosophila* Apaf-1 homolog, Dark. *EMBO J.* 21:2189–2197. doi:10.1093/emboj/21.9.2189

Sato, A., T. Kojima, K. Ui-Tei, Y. Miyata, and K. Saigo. 1999a. Dfrizzled-3, a new *Drosophila* Wnt receptor, acting as an attenuator of Wingless signaling in wingless hypomorphic mutants. *Development.* 126:4421–4430.

Sato, M., T. Kojima, T. Michiue, and K. Saigo. 1999b. Bar homeobox genes are latitudinal prepattern genes in the developing *Drosophila* notum whose expression is regulated by the concerted functions of decapentaplegic and wingless. *Development.* 126:1457–1466.

Sato, K., Y. Hayashi, Y. Ninomiya, S. Shigenobu, K. Arita, M. Mukai, and S. Kobayashi. 2007. Maternal Nanos represses hid/skl-dependent apoptosis to maintain the germ line in *Drosophila* embryos. *Proc. Natl. Acad. Sci. USA.* 104:7455–7460. doi:10.1073/pnas.0610052104

Shapiro, R.S., and K.V. Anderson. 2006. *Drosophila* Ik2, a member of the I kappa B kinase family, is required for mRNA localization during oogenesis. *Development.* 133:1467–1475. doi:10.1242/dev.02318

Takemoto, K., T. Nagai, A. Miyawaki, and M. Miura. 2003. Spatio-temporal activation of caspase revealed by indicator that is insensitive to environmental effects. *J. Cell Biol.* 160:235–243. doi:10.1083/jcb.200207111

Takemoto, K., E. Kuranaga, A. Tonoki, T. Nagai, A. Miyawaki, and M. Miura. 2007. Local initiation of caspase activation in *Drosophila* salivary gland programmed cell death in vivo. *Proc. Natl. Acad. Sci. USA.* 104:13367–13372. doi:10.1073/pnas.0702733104

Tilney, L.G., M.S. Tilney, and G.M. Guild. 1995. F actin bundles in *Drosophila* bristles. I. Two filament cross-links are involved in bundling. *J. Cell Biol.* 130:629–638. doi:10.1083/jcb.130.3.629

Wang, S.L., C.J. Hawkins, S.J. Yoo, H.A. Müller, and B.A. Hay. 1999. The *Drosophila* caspase inhibitor DIAP1 is essential for cell survival and is negatively regulated by HID. *Cell.* 98:453–463. doi:10.1016/S0092-8674(00)81974-1

Williams, D.W., S. Kondo, A. Krzyzanowska, Y. Hiromi, and J.W. Truman. 2006. Local caspase activity directs engulfment of dendrites during pruning. *Nat. Neurosci.* 9:1234–1236. doi:10.1038/nn1774

Wilson, R., L. Goyal, M. Ditzel, A. Zachariou, D.A. Baker, J. Agapite, H. Steller, and P. Meier. 2002. The DIAP1 RING finger mediates ubiquitination of Dronc and is indispensable for regulating apoptosis. *Nat. Cell Biol.* 4:445–450. doi:10.1038/ncb799

Wright, K.M., M.W. Linhoff, P.R. Potts, and M. Deshmukh. 2004. Decreased apoptosome activity with neuronal differentiation sets the threshold for strict IAP regulation of apoptosis. *J. Cell Biol.* 167:303–313. doi:10.1083/jcb.200406073

Yakovlev, A.G., K. Ota, G. Wang, V. Movsesyan, W.L. Bao, K. Yoshihara, and A.I. Faden. 2001. Differential expression of apoptotic protease-activating factor-1 and caspase-3 genes and susceptibility to apoptosis during brain development and after traumatic brain injury. *J. Neurosci.* 21:7439–7446.

Yi, C.H., and J. Yuan. 2009. The Jekyll and Hyde functions of caspases. *Dev. Cell.* 16:21–34. doi:10.1016/j.devcel.2008.12.012

Yoo, S.J., J.R. Huh, I. Muro, H. Yu, L. Wang, S.L. Wang, R.M. Feldman, R.J. Clem, H.A. Müller, and B.A. Hay. 2002. Hid, Rpr and Grim negatively regulate DIAP1 levels through distinct mechanisms. *Nat. Cell Biol.* 4:416–424. doi:10.1038/ncb793

Zachariou, A., T. Tenev, L. Goyal, J. Agapite, H. Steller, and P. Meier. 2003. IAP-antagonists exhibit non-redundant modes of action through differential DIAP1 binding. *EMBO J.* 22:6642–6652. doi:10.1093/emboj/cdg617

Zhang, Y., N. Lin, P.M. Carroll, G. Chan, B. Guan, H. Xiao, B. Yao, S.S. Wu, and L. Zhou. 2008. Epigenetic blocking of an enhancer region controls irradiation-induced proapoptotic gene expression in *Drosophila* embryos. *Dev. Cell.* 14:481–493. doi:10.1016/j.devcel.2008.01.018

Zhou, L., A. Schnitzler, J. Agapite, L.M. Schwartz, H. Steller, and J.R. Nambu. 1997. Cooperative functions of the reaper and head involution defective genes in the programmed cell death of *Drosophila* central nervous system midline cells. *Proc. Natl. Acad. Sci. USA.* 94:5131–5136. doi:10.1073/pnas.94.10.5131